Interfacial polymerization using biobased solvents and their application as desalination and organic solvent nanofiltration membranes

Journal of Membrane Science 692 (2024) 122281

Contents lists available at ScienceDirect

Journal of Membrane Science

journal homepage: www.elsevier.com/locate/memsci

Interfacial polymerization using biobased solvents and their application as desalination and organic solvent nanofiltration membranes

Shiliang Lin [a], Andrea Correa Semiao [a], Yanqiu Zhang [b], Shao Lu [b], Cher Hon Lau [a,*]

[a] School of Engineering, University of Edinburgh, Robert Stevenson Road, EH9 3FK, UK
[b] MIIT Key Laboratory of Critical Materials Technology for New Energy Conversion and Storage, State Key Laboratory of Urban Water Resource and Environment, School of Chemistry and Chemical Engineering, Harbin Institute of Technology, Harbin, 150001, PR China

ARTICLE INFO

Keywords:
Interfacial polymerization
Polyamide thin-film composite
Bio-based solvents
Desalination and organic solvent nanofiltration

ABSTRACT

Thin-film composite membranes are widely regarded as more sustainable technologies for desalination and organic solvent nanofiltration. However, the process of fabricating these membranes is not. This is because n-hexane, a toxic and hazardous solvent, or other fossil-derived oily solvents are used as the organic phase to fabricate polyamide selective layers of such membranes. Here we replaced fossil-derived solvents with benign, bio-renewable solvents that possess better environmental, health and safety metrics – cyclopentyl methyl ether (CPME) and 2-methyltetrahydrofuran (2-MeTHF). A fully aromatic polyamide thin film composite (TFC) membrane fabricated *via* CPME demonstrated a higher NaCl rejection (97.8%), while the same membrane fabricated using n-hexane only presented 92.4% rejection. Meanwhile a semi-aromatic polyamide TFC membrane fabricated with 2-MeTHF showed an ethanol permeance of 9.87 L m^{-2} h^{-1} bar^{-1} and 97.1% RB rejection, 3.7-fold higher than the TFC fabricated using n-hexane. This demonstrated the feasibility and advantages of replacing toxic and hazardous solvents that have long been the standard solvents used in membrane fabrication, with benign alternatives. This work could potentially improve the sustainability of membrane fabrication.

1. Introduction

Ascribing to lower energy requirements, membrane-based separations are typically considered as environmentally sustainable separation technologies [1,2]. For example, in seawater desalination, a distillation-based process consumes 14.45 to 27.25 kWh/m^3 of electricity, compared to consuming 4 to 6 kWh/m^3 for reverse osmosis [3]. This is also valid for solvent recovery where distillation-based processes consume 25–32 times more energy for recovering organic solvents from mixtures compared to organic solvent nanofiltration (OSN) with polymer membranes [4,5]. Most polymer membranes deployed in seawater desalination and organic solvent nanofiltration exist as thin-film composites (TFCs). The most common preparation method of such TFCs is to deposit thin polyamide films as selective layers on porous polymer supports to yield polyamide TFCs for desalination and organic solvent nanofiltration [6,7]. In this process, acyl chlorides e.g. trimesoyl chloride (TMC) is dissolved in a water-immiscible organic solvents such as n-hexane [8], toluene [9] and isoparrafins [10] and interact with diamines such as piperazine (PIP) [11], *m*-phenylenediamine (MPD) [12] dissolved in water. These monomers react with each other at the water-organic solvent interface, forming a polyamide film (Fig. 1). Fully aromatic polyamides such as those containing MPD are preferred for desalination due to higher negative charge [13,14], while semi-aromatic polyamides comprising PIP with lower salt rejection are typically deployed in organic solvent nanofiltration [14,15]. Although the separation process itself is more environmentally sustainable, the process of fabricating polymer membranes is not [16,17]. This is attributed to the use of toxic, hazardous solvents like dimethylformamide (DMF) and n-methyl-2-pyrrolidone (NMP) for fabricating the porous support layer and n-hexane [8], toluene [9] and isoparrafins [10] for the selective layer.

The green metrics of fabricating porous support layers can be improved by reducing the usage of such solvents, or using more benign, bio-based solvents such as Cyrene™ [18] or γ-valerolactone [19]. These strategies have also been deployed to improve the green metrics of fabricating polyamides *via* interfacial polymerization by reducing the usage of, or replacing n-hexane – a fossil-derived solvent that is toxic to aquatic life and potentially damaging fertility [20] with benign, bio-based solvents. For example, Lorena et al. reported a method of vapor phase interfacial polymerization process that eliminated the use

* Corresponding author.
E-mail address: cherhon.lau@ed.ac.uk (C.H. Lau).

https://doi.org/10.1016/j.memsci.2023.122281
Received 24 October 2023; Received in revised form 14 November 2023; Accepted 16 November 2023
Available online 19 November 2023

of organic solvents to yield polyamide membranes with higher nanofiltration permeance reaching 3.3 L m^{-2} h^{-1} bar^{-1} with 94 % rejection rates [21]. But this method also prolonged the reaction time from 1 min to at least 30 min for acyl chloride vapor diffusion. Jose et al. employed a similar vapor interfacial polymerization approach that avoided using any organic solvent, but the resultant polyamide TFC present a 20 % lower water permeance [22]. Tang and co-workers [23] also reported such zero-organic-solvent vapor polymerization approach and the resultant PIP-TMC TFC showed a rejection of 96.2% against Na_2SO_4 and permeance of 6.8 L m^{-2} h^{-1} bar^{-1}, but this method required 20 hours of synthesis time. Ma et al. reduced the amount of organic solvents used during membrane fabrication *via* electrospraying [24]. However, the resultant polyamide membrane was only suitable for heavy metal ion removal. Ong et al. replaced n-hexane with decanoic acid, a plant-based fatty acid, during interfacial polymerization of polyamide-based selective layers, yielding membranes with water and isopropanol permeances of 52 and 16 L m^{-2} h^{-1} bar^{-1}, respectively [25]. Although this approach yielded polyamide-based TFC membranes with exemplary separation performances, a more costly polyamine (polyethyleneimine) was used.

Other potential alternative solvents for n-hexane include cyclopentyl methyl ether (CPME), a fossil fuel-derived solvent that can be potentially produced from bio-derived adipic acid and furfurals [26], and 2-methyltetrahydrofuran (2-MeTHF) [27] which could be synthesized from various biomasses. These solvents have low miscibility with water and can dissolve chemicals used in polyamide synthesis like TMC [26], hence are ideal for interfacial polymerization. Moreover, the strategy of using CPME and 2-MeTHF to replace incumbent solvents for processing has also been demonstrated for carotenoids extraction [28,29], solar cells production [30,31], amides coupling [32], biodiesel purification [33] and dimethindene synthesis [34]. These works indicated the possibility of using CPME or 2-MeTHF as the organic solvent for interfacial polymerization. Potential advantages of CPME and 2-MeTHF over n-hexane and toluene for interfacial polymerization are their lower peroxide risks and energy footprints during solvent production. CPME and 2-MeTHF are also ranked as "useable", "preferred" and "some issues" by major pharmaceutical companies [26,35,36]. Both solvents compare favorably with n-hexane, toluene and isoparaffins – incumbent solvents deployed in interfacial polymerization of polyamide selective layers.

Here we hypothesised that n-hexane can be replaced with alternative solvents that are more benign – CPME and 2-MeTHF during interfacial polymerization of polyamides. This hypothesis is based on the better green metrics of CPEM and 2-MeTHF when compared to n-hexane [26,27] and their deployments to replace oily fossil-derived solvents [28–33]. To validate this hypothesis, we attempted to fabricate a variety of polyamides using CPME- and 2-MeTHF-based solutions. Complementary experiments and characterization techniques deployed here in this work validated the hypothesis of our approach. As the separation performances of polyamides synthesized using these solvents outperformed those fabricated using n-hexane, outcomes from this work may potentially improve the sustainability of TFC membrane fabrication and other processes that require interfacial polymerization.

2. Experimental

2.1. Materials and equipment

Polyethersulfone (E3020P) was kindly provided by BASF, Germany. Cyrene™ was purchased from Circa Group Ltd, Parkville, Australia. 2-methyltetrahydrofuran (2-MeTHF), cyclopentyl methyl ether (CPME), Rose Bengal dye (RB, 1017.64 g mol^{-1}), Piperazine (PIP, >99.0 %), *m*-phenylenediamine (MPD, >99.5%), *p*-phenylenediamine (PPD), 1,6-diaminohexane (DH) and 1,3-cyclohexanebis(methylamine) (CMA) were purchased from Sigma Aldrich. Trimesoyl chloride (TMC, 98+ %) was purchased from Alfa Aesar. n-hexane and ethanol (EtOH, 99.99 % purity) were from Fisher Chemicals.

An automated spray-coating machine adapted from a commercial 3D-printer was used here to fabricate the porous support layers. Details of this machine can be found in our previous work [37].

2.2. Interfacial polymerization with n-hexane and bio-based solvents

First, 2 wt% of amines (PIP, MPD, PPD, DH and CMA) were dissolved in deionised water, while conventional 0.2 wt% of TMC was dissolved in n-hexane and 0.2, 1 and 3 wt% of TMC were dissolved in two sets of separate vials, each containing CPME or 2-MeTHF. The reasons for choosing various TMC concentrations are explained in the Results and Discussion session. Free-standing PA films were fabricated by interfacial polymerization at the water-organic solvent interface. Briefly, 50 ml of amine water solution was allowed to rest in a glass Petri dish, a lifting

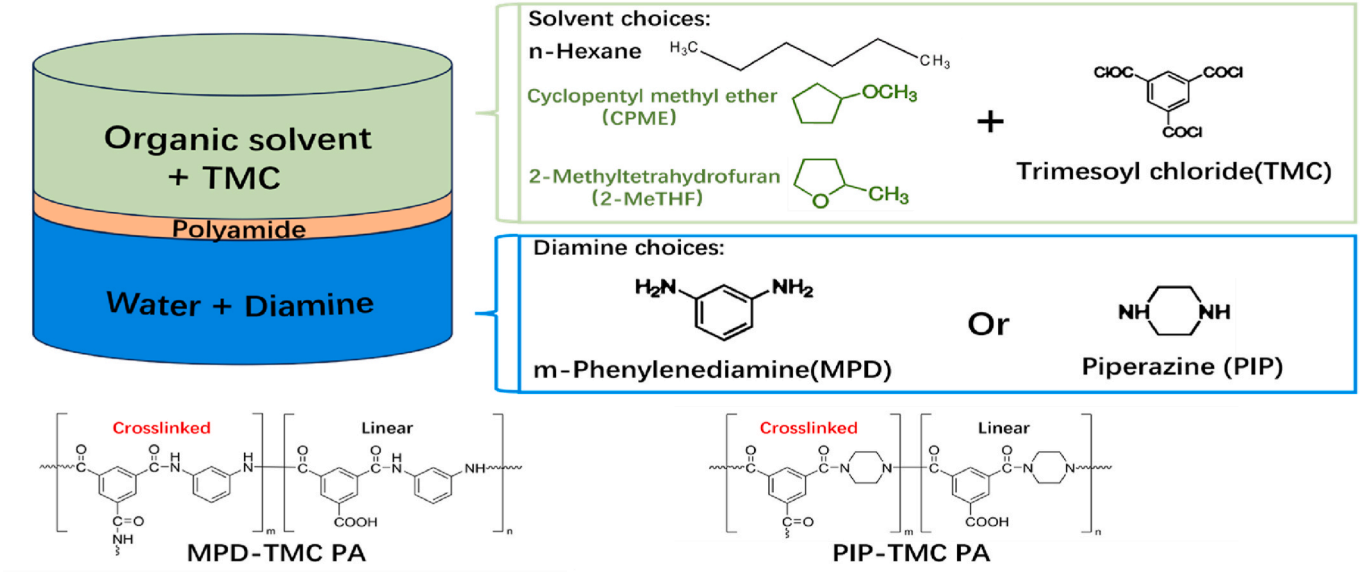

Fig. 1. The proposed bio-based organic solvents and chemical structure of polyamides. Different from the conventional organic solvent like n-Hexane, more benign solvents such as CPME and 2-MeTHF were deployed to dissolve TMC. Aromatic diamine (MPD) and aliphatic diamine (PIP) were used for preparation of fully aromatic polyamide and semi-aromatic PA, respectively. The resultant polyamides comprised by both crosslinked and linear structures.

tool with a stainless-steel mesh installed was immersed in the water-amine solution (Fig. S1). Then 50 ml of a TMC organic solution was poured slowly on top of the amine water solution. The reagents were allowed to react for 5 min. Once the interfacial polymerization was completed, the lifting tool will be slowly and vertically lifted, and the polyamide thin film will be landed on top of the mesh woven. Then this lifting tool will be slowly and vertically transferred to water bath and the polyamide thin film was floated on surface of the water bath to remove residual amine and fully terminate the interfacial polymerization reaction (Fig. S1). The free-standing PA films were stored in deionised water until further characterization with FTIR and XPS.

2.3. Fabrication of PES porous supports using a more benign, bio-based solvent via spray coating

The porous support layers for the TFC membranes studied here were fabricated using (Cyrene™) [38] *via* spray coating. We chose to use PES support layers fabricated from this approach to demonstrate the feasibility of fabricating the entire structure of TFC membranes – selective layer and porous support from more benign, bio-based solvents.

Briefly, PES dope solutions were prepared by dissolving 15 wt% PES and 1 wt% PVP i.e., porogen in Cyrene™ at 80 °C. This dope solution was stirred magnetically until complete PES dissolution, forming a viscous and transparent solution. This dope solution was loaded into the solution reservoir of a spray gun. Spraying distance was set to 20 cm above a glass plate placed on the build plate of the 3D printer. The build plate was not heated prior and throughout spray coating. 4 bar of nitrogen was supplied to the spray gun and spray gun movement was controlled by the control circuit and stepper motors. The spray gun moved across the glass plate to ensure full coverage of the printing area. This process was repeated for 6 times at room temperature to produce a PES film with thickness around 200 μm. After the dope solution was coated on top of glass plate, the glass plate was immersed immediately into a coagulation bath, forming a PES support upon non-solvent induced phase separation. The resultant PES supports were stored in pure water at room temperature until further procedures were needed. The pure water permeance of this spray coated PES support was 63.7 L m^{-2} h^{-1} bar^{-1}.

2.4. Fabrication of TFC polymer membranes using n-hexane, CPME and 2-MeTHF

Based on results from experiments on synthesising free-standing PA, we only selected specific combinations of amine and TMC concentrations that can form a PA film for TFC fabrication (Fig. S2). For desalination applications, MPD-TMC PA TFC membranes were prepared by both n-hexane and bio-based solvents as organic solvent. For OSN applications, PIP-TMC PA TFC membranes were prepared by both n-hexane and bio-based solvents.

Briefly, PES membranes fabricated from spray coating were used as porous support layers for all TFCs. A PES membrane was taped to a glass plate, with the top surface facing upwards and placed in an aqueous solution comprising 2 wt% MPD or PIP for 5 min. The amine-loaded PES support was removed from the solution and pressed with a roller to remove excess amine solution, prior to immersion in organic solutions. For n-hexane, the TMC concentration was set at 0.2 wt%, and for CPME and 2-MeTHF the TMC concentrations were 3 wt%. This is due to the PA layer formation ability and crosslinking degree, detailed reasonings of this concentration setting will be explained in result and discussion session below. The resultant TFCs were placed in an oven at 50 °C for 5 min and washed gently with water to remove unreacted and residue amine and TMC.

2.5. Membranes characterization

The surface and cross-section morphologies of membrane samples studied here were observed with a Carl Zeiss SIGMA HD VP Field Emission Scanning Electron Microscopy (FE-SEM). All samples were dried for 12 h in a vacuum oven before SEM analysis. For cross-section SEM characterization, membrane samples were first freeze-fractured in liquid nitrogen. A 10 nm-thin layer of gold was sputter-coated on to the samples before imaging. An accelerating voltage of 5 kV was used to obtain SEM micrographs.

FTIR was performed in attenuated total reflectance (ATR) mode on a Nicolet™ iS™ 20 FTIR Spectrometer (Thermo Scientific™) with a Smart iTX™ diamond accessory to characterise functional groups over a range of 500–4000 cm^{-1}. XPS Analysis was performed using a Kratos Axis SUPRA XPS fitted with a monochromated Al kα X-ray source (1486.7 eV), a spherical sector analyser and 3 multichannel resistive plate, 128 channel delay line detectors. All data was recorded at 150W and a spot size of 700 × 300 μm. Survey scans were recorded at a pass energy of 160 eV, and high-resolution scans recorded at a pass energy of 20 eV. Electronic charge neutralization was achieved using a magnetic immersion lens. Filament current = 0.27 A, charge balance = 3.3 V, filament bias = 3.8 V. All sample data was recorded at a pressure below 10^{-8} Torr and at 150 K temperature. Data was analysed using CasaXPS v2.3.20PR1.0 and the spectra were calibrated with C1s peak at 284.8 eV. UPS measurements were performed with He I (21.2 eV) radiation source. Each PA sample's Atom% was calculated using the CasaXPS software and the crosslinking degree in each type of polyamide was calculated using the following equations (1)-(3):

$$\frac{O}{N}=\frac{3m+4n}{3m+2n} \tag{1}$$

$$m+n=1 \tag{2}$$

$$Crosslinking\ degree=\frac{m}{m+n} \tag{3}$$

where O/N is the atomic ratio of polyamide, m and n are the portion of crosslinked and linear parts. All samples were dried for 12 h in a vacuum oven before analysis. AFM topography images of the PES support and polyamide TFC membranes were obtained using a Nanoscope IIIa Multimode scanning probe microscope (Bruker AXS Inc) with an E-scanner in tapping mode using silicon cantilevers. No other image processing was applied except flattening, which was performed here using Gwyddion.

2.6. Desalination and OSN testing

The pure water and solvent permeances of the PES and TFC membranes were measured using triplicate samples and a Sterlitech stainless steel HP4750 stirred dead-end cell. The feed solution comprised deionised water obtained from a lab-based water purification system and pressurized with nitrogen gas at 1 bar at room temperature to reach steady flow rate, then measured at 3 bars. During filtration, the feed solution was stirred at 400 rpm. Permeate samples were collected in capped flasks as a function of time, weighed, and analysed. The permeance was calculated using the following equation (4):

$$Permeance=\frac{V}{At\Delta P} \tag{4}$$

where permeance (L m^{-2} h^{-1} bar^{-1}) is expressed in terms of V, the volume of the solvent passing through the membrane (L), A – effective membrane area (m^2), t – operation time (h), and ΔP – the applied pressure (bar).

The salt rejection rates of TFC membranes were determined using a 2000 ppm NaCl water solution as feed solution and stirred at 400 rpm to avoid concentration polarization. The feed solution was pressurized at 3 bar to reach a steady flow rate and measured at 3 bars. The feed and permeate salt concentrations were determined by measuring water conductivities with a Thermo Scientific Orion Star A212 benchtop

Conductivity Meter. Rejection rates of the TFC membranes were calculated using the following equation (5):

$$Rejection\ rate = \left(1 - \frac{C_p}{C_f}\right) * 100 \quad (5)$$

where C_p and C_f are the solute concentrations in the permeate and feed solution, respectively.

For OSN testing, the solvent permeance of the composite membranes were measured using a stainless-steel dead-end pressure cell. Feed solutions were prepared using common chemicals – EtOH and a dye Rose Bengal (RB) with a molecular weight of 1017.64 g mol^{-1}. The feed solution was pressurized with nitrogen gas at 3 bars at room temperature. During filtration, the feed solution was stirred at 400 rpm to avoid concentration polarization. Permeate samples were collected in capped flasks as a function of time, weighed, and analysed. The permeance was calculated using equation (4), but V is the volume of the solvent passing through the membrane (L), while other parameters were the same as desalination test.

The selectivities of the membranes were calculated using equation (5), where C_p and Cf are the solute concentrations in the permeate and feed solution, respectively. Dye concentrations in the solvents were measured using UV-VIS spectrometry (Evolution 60, Thermo Scientific). Each data point is an average of three repetitions of each test.

3. Results and discussion

3.1. TMC concentration choices for bio-based solvents

Identical to previous reports [39–42], a distinctive polyamide layer was formed at the interphase of water and hexane solutions containing 2 wt% amines and 0.2 wt% TMC, respectively, *via* interfacial polymerization, (Figs. S2a and i). However, here we did not observe a distinctive polyamide layer when a CPME or 2-MeTHF solution containing 0.2 wt% TMC was used (Figs. S2b and j). Polyamide was only formed at the interfaces of water-CPME and water-MeTHF solutions when TMC content reached 3 wt%. This could be attributed to the higher water solubilities of CPME (11 g L^{-1}) [26,43] and 2-MeTHF (40 g L^{-1}) [26,43] when compared to n-hexane (9.5 mg L^{-1}). Higher water solubilities of CPME and 2-MeTHF meant that diamine molecules in water could diffuse more easily into the organic phase containing TMC and react with TMC at the interface and in the bulk organic phase [44,45]. Interfacial polymerization of polyamide is a self-limited reaction where the initial formation of a polyamide film acts like a barrier to slow down subsequent growth of the polyamide film [46,47]. Without this dense barrier at the initial stages of interfacial polymerization, as per the cases of CPME and 2-MeTHF, the diffusion of diamine into the bulk organic phase will not be hindered. Hence forming polyamide within the bulk organic phase. This was also why we only observed a cloudy organic phase that did not contain any polyamide film at the CPME-water or 2-MeTHF-water interfaces when TMC content was between 0.2 and 1 wt% (Figs. S2b, f, j and m).

A potential solution to address this limitation is to increase TMC content in the organic phase [48], where 2 wt% of diamines reacted with 3 wt% of TMC, 15-fold more than the well-reported TMC concentration of 0.2 wt% [37], led to formation of a dense initial polyamide film. This was also observed here in this work when TMC content in CPME and 2-MeTHF reached 3 wt%. Based on these results, when using CPME and 2-MeTHF to fabricate TFC membranes, the concentration of TMC in such solvents was set at 3 wt%.

3.2. Chemical analysis of free-standing polyamide films

The chemical structures of the five polyamide types fabricated using various diamines and TMC dissolved in n-hexane, CPME and 2-MeTHF where characterised with ATR-FTIR (MPD-TMC and PIP-TMC in Fig. 2, and the rest polyamides in Fig. S3) and XPS (Figs. S4–6). Typical of semi-aromatic polyamides [39,40], the FTIR spectra of this class of polyamides studied here, namely PIP-TMC, DH-TMC, and CMA-TMC comprised a peak at 1625 cm^{-1} that could be ascribed to the C=O stretching vibration [39,40]. Meanwhile, from the FTIR spectra of fully aromatic polyamides studied here, i.e., MPD-TMC and PPD-TMC, we also observed peaks that correlate to the amide I, aromatic amide and amide II bands at 1665 cm^{-1}, 1611 cm^{-1} and 1544 cm^{-1}, respectively [41,49]. The FTIR spectra of all 5 polyamides studied here confirmed that replacing n-hexane with CPME or 2-MeTHF did not affect the general chemical composition of polyamides.

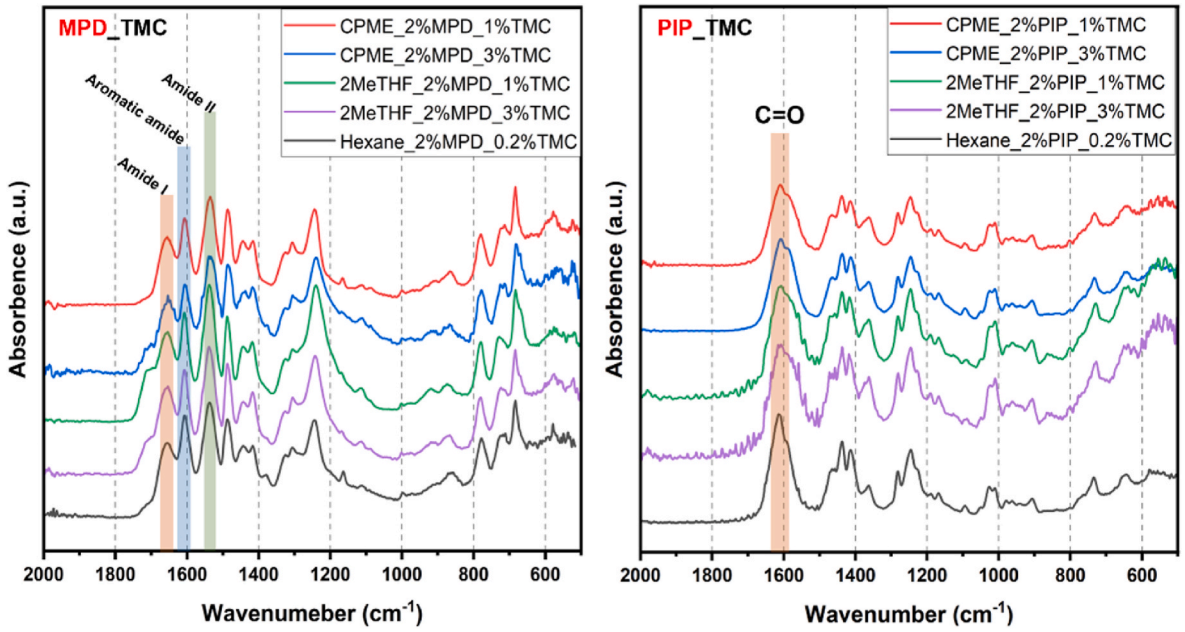

Fig. 2. ATR-FTIR of MPD-TMC and PIP-TMC PA fabricated using n-hexane, CPME and 2-MeTHF.

The atomic percentages of oxygen, carbon and nitrogen of all polyamides studied here (Table 1) were determined using XPS survey scans and Equations (1)–(3). Since some combinations of amine and TMC did not form a polyamide film, those combinations were not listed in Table 1. The theoretical O/N ratio of a fully crosslinked polyamide (with 100% crosslinking degree) is 1.0, whereas the O/N ratio of a linear polyamide chain (with 0 % crosslinking degree) is 2.0 [40]. Here, the O/N ratio of a fully aromatic polyamide produced via interfacial polymerization of 2 wt% MPD and 0.2 wt% TMC in n-hexane was 1.37, with a crosslinking degree of 52.4 %. As n-hexane was replaced with CPME or 2-MeTHF, the amount of TMC used in interfacial polymerization increased from 0.2 wt% to 3 wt%. This reduced O/N ratio values by 16.8 % and 6.6 %, reaching 1.14 and 1.28 when CPME and 2-MeTHF were used respectively. These reduction in O/N ratio also increased the crosslinking degree in MPD-TMC polyamide produced with CPME or 2-MeTHF as organic solvents, to 79.9 % and 62.2 %, respectively. Similar improvements in crosslinking degree upon the increase of TMC concentration were reported when using toluene and xylene as organic solvents [44]. These trends were also observed with semi-aromatic polyamides studied here. The O/N ratio and crosslinking degree of a semi-aromatic polyamide, such as PIP-TMC, synthesized using n-hexane as the organic phase comprising 0.2 wt % TMC and 2 wt% PIP in water were 1.16 and 77.17 %, respectively. After replacing n-hexane with CPME or 2-MeTHF, the crosslinking degree in PIP-TMC increased to 77.57 % and 84.92 %, respectively.

XPS C1s high-resolution scans (Fig. S6) validated that replacing n-hexane with CPME and 2-MeTHF as the organic phase in interfacial polymerization did not affect the formation of polyamides. Regardless of the organic phase deployed, here we observed the same type of peaks that corresponded to O=C-O (~288.5eV), O=C-N (~287.9eV), C-N (~285.6eV) and C-C/C-H (~284.7eV) in fully aromatic MPD-TMC polyamide [50,51]. However, the amount of each of these functional groups varied as a function of crosslinking degree in the polyamides. As shown in Fig. 1, the O=C-N group was formed *via* an amide-forming reaction between an acyl chloride of TMC and amine groups of MPD or PIP, while an O=C-O group was formed by hydrolysis of unreacted acyl chlorides in TMC monomers [50–52]. Variation in O=C-N and O=C-O content was in line with crosslinking degree calculations. With a crosslinking degree of 52.39 % in MPD-TMC polyamides yielded with n-hexane, the C=O-O and O=C-N content (calculated by deconvolution of XPS carbon spectrum) reached 2.7 % and 9.9 %, respectively. The replacement of n-hexane with CPME increased the crosslinking degree in resultant MPD-TMC polyamides to 79.9 %, but reduced O=C-O content to 2.1 % and increased O=C-N to 12 %. This indicated that the proportion of crosslinked structure increased while the proportion of linear structure decreased [50,52]. This showed that crosslinking between TMC and MPD was more prevalent in CPME, possibly due to an improved solubility in water when compared to n-hexane [44] and the increased amount of TMC in CPME. When using organic solvent with higher water solubility, the diffusion of MPD will be accelerated and more MPD molecules can react with TMC to form a more crosslinked structure [44,45]. On the other hand, increasing the TMC concentration also led to increase in reaction rate and a higher crosslinking degree [48]. Similar trends could also be observed in the XPS spectra of the semi-aromatic polyamide of PIP-TMC [53,54] where the replacement of n-hexane with 2-MeTHF during interfacial polymerization increased the O=C-N content in PIP-TMC polyamide from 9.1 % to 12.5%, while reducing O=C-O content from 4.1 % to 1.5 %, and the final crosslinking degree increased from 77.17% to 84.92%.

3.3. Surface morphology of polyamide – PES TFCs

All polyamide-TFC membranes in this study were fabricated by depositing polyamide films onto the surfaces of porous PES supports via interfacial polymerization. Amine concentrations in water were set at 2 wt% for both fully aromatic MPD-TMC polyamide and semi-aromatic PIP-TMC polyamide. Depending on solvent choice, TMC content in n-hexane was fixed at 0.2 wt% and 3 wt% in both CPMD and 2-MeTHF. SEM images of the pristine PES porous support is showed in Fig. S7, and SEM images of all TFCs were shown in Figs. 3 and 4.

From SEM micrographs in Fig. 3a, we observed that the surface morphology of MPD-TMC fabricated using n-hexane comprised of crumpled ridges and valleys. This could be attributed to the uneven distribution of interfacial polymerization reaction heat [42,55].

Table 1
Atomic percentages, O/N ratio and crosslinking degree of each polyamide sample.

Solvent type	Diamine_wt.%	TMC_wt.%	Atomic composition (At%)			O/N ratio	Crosslinking degree (%)
			C	O	N		
n-hexane	MPD_2%	TMC_0.2%	73.54	15.33	11.13	1.38	52.39
	PIP_2%	TMC_0.2%	75.97	12.93	11.10	1.16	77.17
CPME	MPD_2%	TMC_0.2%	80.66	11.22	8.12	1.38	52.04
	MPD_2%	TMC_1%	79.39	11.64	8.97	1.30	61.15
	MPD_2%	TMC_3%	78.24	11.61	10.15	1.14	79.94
	PIP_2%	TMC_1%	75.31	15.05	9.64	1.56	34.36
	PIP_2%	TMC_3%	75.98	12.91	11.11	1.16	77.57
	DH_2%	TMC_0.2%	87.54	7.13	5.33	1.34	56.66
	DH_2%	TMC_1%	78.25	12.30	9.45	1.30	60.65
	DH_2%	TMC_3%	75.86	13.56	10.58	1.28	62.98
	CMA_2%	TMC_1%	77.33	13.91	8.76	1.59	31.76
	CMA_2%	TMC_3%	76.96	13.91	9.13	1.52	37.78
	PPD_2%	TMC_0.2%	76.66	14.11	9.62	1.47	43.20
	PPD_2%	TMC_1%	75.42	14.13	10.45	1.35	55.04
	PPD_2%	TMC_3%	76.37	13.11	10.52	1.25	67.01
2MeTHF	MPD_2%	TMC_1%	77.69	13.23	9.08	1.46	44.14
	MPD_2%	TMC_3%	80.41	11.03	8.56	1.29	62.20
	PIP_2%	TMC_1%	74.61	15.40	9.99	1.54	36.12
	PIP_2%	TMC_3%	79.04	11.01	9.95	1.11	84.92
	DH_2%	TMC_0.2%	77.54	13.62	8.84	1.54	36.25
	DH_2%	TMC_1%	78.02	12.80	9.18	1.39	50.64
	DH_2%	TMC_3%	79.98	11.53	8.49	1.36	54.46
	CMA_2%	TMC_1%	77.84	14.02	8.14	1.72	20.30
	CMA_2%	TMC_3%	77.51	13.30	9.19	1.45	45.10
	PPD_2%	TMC_1%	76.69	14.00	9.31	1.50	39.65
	PPD_2%	TMC_3%	76.33	13.80	9.87	1.40	50.15

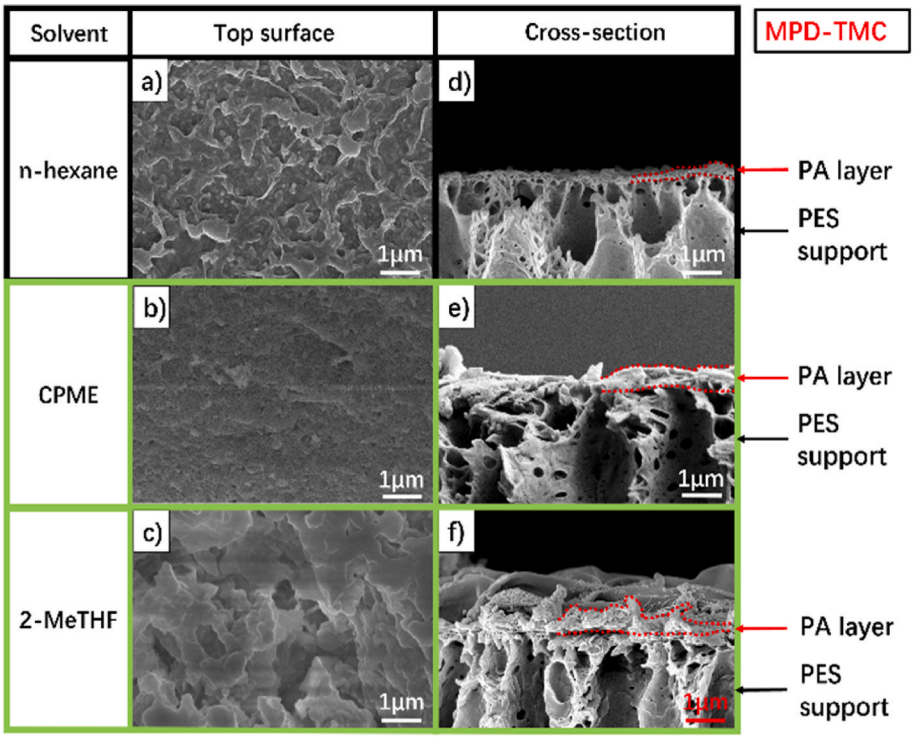

Fig. 3. SEM images of PES-MPD-TMC polyamide TFC membranes. a and d) Top surface morphology and cross-section SEM images of MPD-TMC polyamide TFC fabricated using n-hexane as organic solvent; b and e) MPD-TMC Polyamide TFC fabricated using CPME as organic solvent; c and f) MPD-TMC Polyamide TFC fabricated using 2-MeTHF as organic solvent.

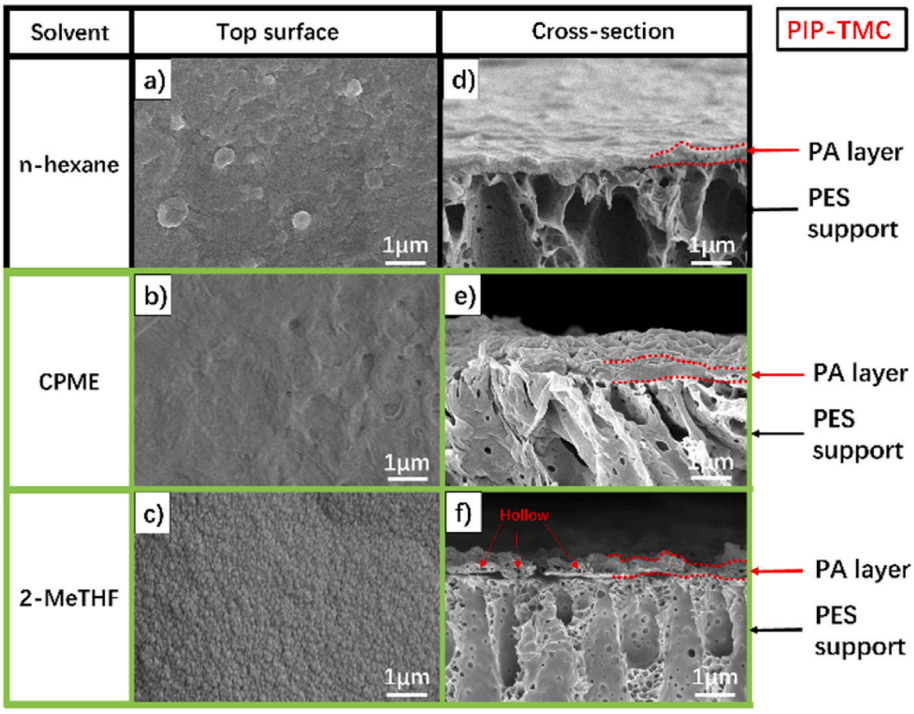

Fig. 4. SEM images of PES-PIP-TMC polyamide TFC membranes. a and d) Top surface morphology and cross-section SEM images of PIP-TMC polyamide TFC fabricated using n-hexane as organic solvent; b and e) PIP-TMC Polyamide TFC fabricated using CPME as organic solvent; c and f) PIP-TMC Polyamide TFC fabricated using 2-MeTHF as organic solvent.

Replacing n-hexane with CPME (Fig. 3b) and 2-MeTHF (Fig. 3c) as the organic phase during interfacial, we observed that the surfaces of resultant polyamide layers comprised of aggregate-like features. This could be ascribed to the CPME/water and 2-MeTHF/water solubility differences. Kong et al. demonstrated that the presence of 2 wt% acetone in the n-hexane organic phase enhanced the solubility of water in

n-hexane-acetone when compared to a binary mixture of water/n-hexane [56]. Consequently, the presence of acetone doubled the MPD diffusion rate into the organic phase, resulting in aggregated surface features [57]. Park et al. evaluated the impact on the interfacial polymerization mechanism while using more water-soluble solvents as organic phase [44]. In their study, n-hexane was replaced with xylene or toluene. The replacement solvents were more miscible with water, resulting in a thick miscible interface where MPD and TMC coexisted. This was favourable for interfacial polymerization. The surfaces of polyamides fabricated using toluene (solubility in water = 526 mg L^{-1}) comprised polyamide fragments that were stacked higher and aggregated into bigger nodule compared to those fabricated using xylene (solubility in water = 180 mg L^{-1}). This was also reported elsewhere when other type of organic phase additives [58,59] were used, or when ionic liquids were deployed as the organic phase [60]. Here in this work, the organic solvents used were more soluble in water where the water solubilities of CPME and 2-MeTHF reached 11 and 40 g L^{-1}, respectively. This was also why we observed higher stacks and larger nodules of polyamide on the surface of MPD-TMC polyamide fabricated using 2-MeTHF (Fig. 3c and f). The higher water solubilities of CPME and 2-MeTHF and requirement of more TMC in these solvents also increased the polyamide layer thickness to ~500 and ~1000 nm, respectively (Fig. 3e and f).

Similar to reports elsewhere [61–63], we also observed the crumpling phenomenon on the surfaces of PIP-TMC polyamide films yielded from n-hexane (Fig. 4a). Fang et al. showed that inhibition of PIP (amine) diffusion towards the organic phase can limit the growth of the polyamide layer, thus reducing its thickness [63]. Meanwhile, if the diffusion of reactants was enhanced, the surfaces of resultant polyamide layers from interfacial polymerization would be rougher [64]. Wang et al. demonstrated that PIP diffusion in toluene was 32-fold faster than in hexane, accelerating and promoting interfacial polymerization between PIP and TMC [65]. We also observed these trends (Fig. 4a-c), when n-hexane was replaced with more water-soluble solvents of CPME and 2-MeTHF, the polyamide surfaces become rougher. It has been reported that the partition coefficient of PIP is much lower than that of MPD [14]. This inferred with the same concentration and liquid-liquid interfaces, PIP diffusion from aqueous phase to organic phase would be slower than that of MPD. Hence the changes in thickness of PIP-TMC polyamide fabricated using n-hexane (150 nm), CPME (250 nm) and 2-MeTHF (400 nm) were less pronounced than those observed in MPD-TMC polyamide films (Fig. 4d-f). We also observed that roof-like hollow structures were formed when the most water-miscible solvent, 2-MeTHF, was used as the organic phase during interfacial polymerization, such features could enhance solvent permeance of resultant PIP-TMC polyamide [14,44].

Surface roughness is one of the key features that can partially determine the final membrane performance [42,44,55,59,64]. Higher surface roughness can provide larger active area [59,64] and bigger pore size [66] for water permeation, but this also means that the membrane is more vulnerable to fouling where permeances will inadvertently be reduced [67]. In this work, we characterised the surface roughness (root mean square, RMS) of both the pristine PES support and all polyamide TFC membranes using an AFM (Fig. 5). The surface roughness of

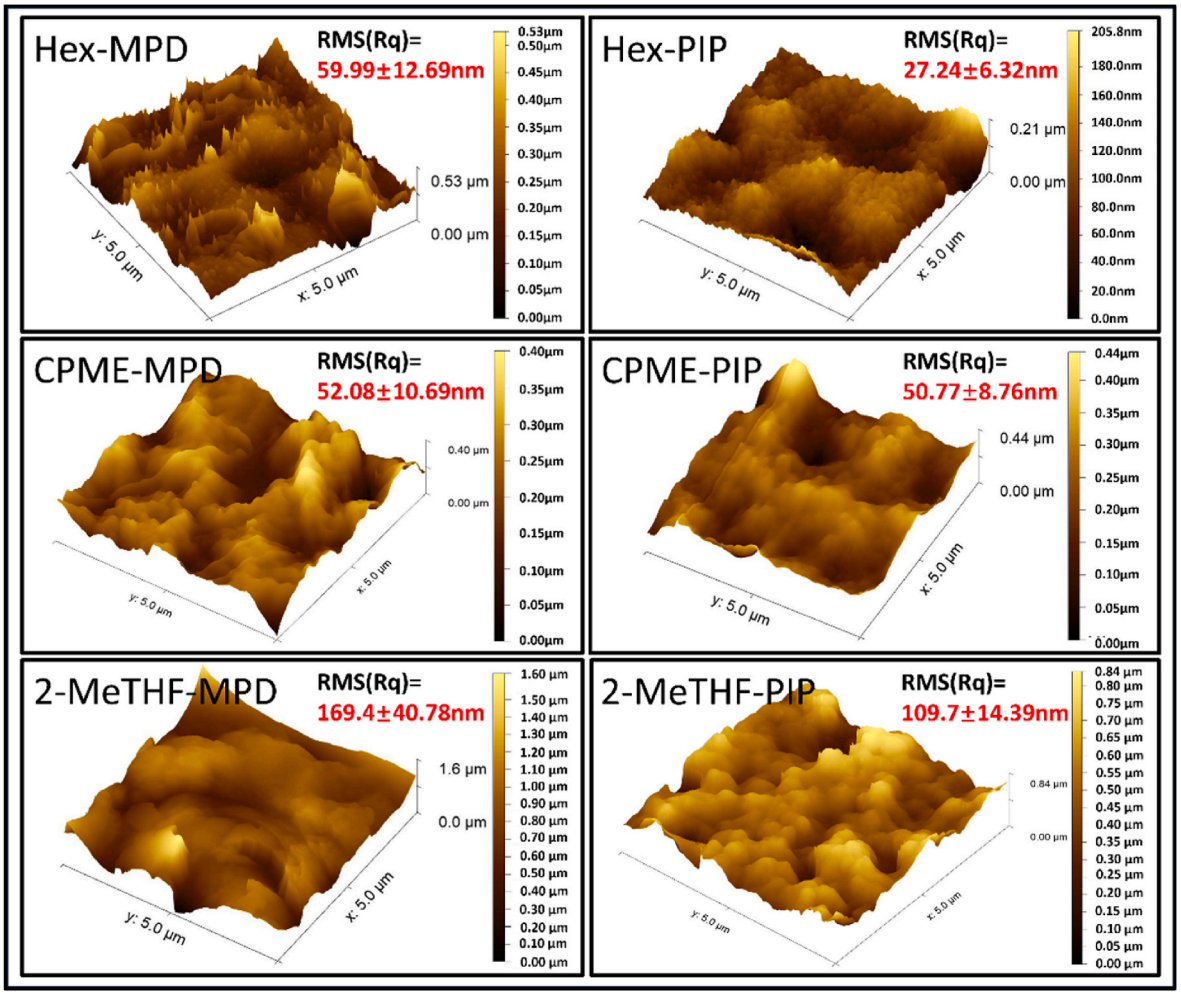

Fig. 5. AFM scans of MPD-TMC (left) and PIP-TMC (right) polyamide TFC membranes.

MPD-TMC polyamide film fabricated using n-hexane reached 59.99 ± 12.69 nm. This was identical to similar polyamide films reported elsewhere [15,68]. The surface roughness of MPD-TMC polyamide was slightly reduced to 52.08 ± 10.69 nm when CPME was used as organic phase during interfacial polymerization. This was in line with its corresponding SEM micrograph (Fig. 3b and e), where we did not observe any ridge and valley structures. The surface of MPD-TMC polyamide fabricated with 2-MeTHF as organic solvent was the roughest amongst all membranes studied here, reaching a RMS value of 169 ± 40.78 nm. As shown in Figure 3c and f, this surface roughness was attributed to the high stacks and large nodules of polyamide. Meanwhile, for PIP-TMC polyamides, we observed that the surface roughness of these films increased from 27.24 ± 6.32 nm to 50.77 ± 8.76 nm and 109.7 ± 14.39 nm as we switched the organic phase from n-hexane to CPME and to 2-MeTHF. The surface roughness of our PIP-TMC film derived from n-hexane was comparable to those reported elsewhere [63]. The changes in surface roughnesses of PIP-TMC polyamide films as a function of solvent water miscibility correlated to the morphological changes observed from SEM microscopy (Fig. 4).

3.4. Desalination and OSN filtration test

Fully aromatic polyamides such as MPD-TMC are mostly deployed as the selective layer of TFC membranes for desalination due to its higher charge repulsion [13]. Meanwhile TFC membranes comprising semi-aromatic PIP-TMC selective layers are mostly studied for OSN [15]. For desalination against a 2000 ppm NaCl water solution, TFC membranes comprising MPD-TMC polyamide selective layers fabricated using n-hexane, the permeance reached 1.76 L m^{-2} h^{-1} bar^{-1}, while NaCl rejection rate reach 92.4% [37]. The replacement of n-hexane with CPME as the organic phase deployed in interfacial polymerization of the MPD-TMC enhanced the TFC membrane salt rejection to 97.8%, mainly due to the increase of crosslinking degree (from 52.39% to 79.94%). It is suggested that the increase of crosslinking degree led to a higher rejection rate but lower permeance [13,42,69]. Together with the fact that the polyamide thickness fabricated by CPME remain at similar level of polyamide fabricated by n-hexane (Fig. 3), we observed a decrease of permeance from 1.76 to 1.51 L m^{-2} h^{-1} bar^{-1} (Fig. 6). But when we switched the organic solvent from n-hexane to 2-MeTHF, we observed a decrease in both water permeance and rejection due to the 4-fold increase in thickness of polyamide layer (Fig. 3) and decrease of crosslinking degree (Table 1).

In terms of OSN performance of semi-aromatic PIP-TMC polyamide TFC membrane, when using conventional n-hexane as organic solvent, TFC membranes demonstrated RB rejection rates of 94.5% in EtOH, and permeance of 2.67 L m^{-2} h^{-1} bar^{-1}. The separation performances of PIP-TMC polyamide TFC membranes were comparable to other TFC membranes reported in literature [61,70]. Meanwhile, switching the organic solvent to CPME led to lower permeance and lower rejection due to the decrease of crosslinking degree (Table 1) and a 166.7% increase of polyamide layer thickness (Fig. 4), but switching the organic solvent to 2-MeTHF gave a 367% increment in EtOH permeance to the PIP-TMC polyamide TFC membrane, reaching 9.87 L m^{-2} h^{-1} bar^{-1}, accompanied by an RB rejection increase to 97.1%. The improvement of permeance and rejection can be ascribed to the increase of crosslinking degree and its loose and roof-like structure. It was reported that higher crosslinking degree led to a more negatively charged membrane surface [71–73] that can provide better charge repulsion against negatively charged dye (RB) [71–74]. Beside crosslinking degree, the roof-like loose polyamide structure also plays an important role in the improvement of permeance. In previous publications, loose polyamide selective layers have been shown to improve both rejection and permeance performance [44], with a similar loose structure providing a lower hydraulic resistance [73,75] and higher permeance (Fig. 6).

Comparison to other RO desalination and OSN membranes is shown in Table 2. When using conventional n-hexane or isoparrafins as organic solution, the permeance and rejection are similar due to the formation of identical fully aromatic polyamide selective layer [76,77]. When switching to toluene, xylene, CPME and ionic liquids as organic solutions, due to the mutual miscibility of these solvents with water, the diffusion rates of MPD into these organic solutions follow the order of water-organic interfacial tension [44,66,67,78]. The lower the water-organic interfacial tension, the quicker diffusion will take place, forming denser polyamide layer. The interfacial tension order from low to high is ionic liquid < CPME < xylene < toluene, this is in line with the increment of permeance and rejection for polyamide TFC fabricated with these organic solvents.

On the other hand, for PIP-TMC polyamide TFC membranes, when using the conventional fabrication approach, the RB rejection and EtOH permeance were similar to literature [71]. The PIP-TMC polyamide TFC membrane fabricated in this study via using 2-MeTHF demonstrated a better EtOH permeance with comparable RB rejection. This was mainly due to the loose and hollow structure of polyamide selective layer. Similar improvement was also reported by Cheng et al., where the incorporation of UiO-66 nanoparticles enhanced the intrinsic porosity of the selective layer [83] where resultant TFC membranes presented a triple rose Bengal permeance increment without sacrificing the rejection. Similar strategy was also reported for RO TFC membrane where mesoporous polymer nanospheres were introduced to double the water permeance [85], reaching 3.75 L m^{-2} h^{-1} bar^{-1} with 98.7% NaCl rejection rate. The interconnected mesoporous channels can increase the overall porosity of the selective layer, giving the TFC high permeance and high rejection.

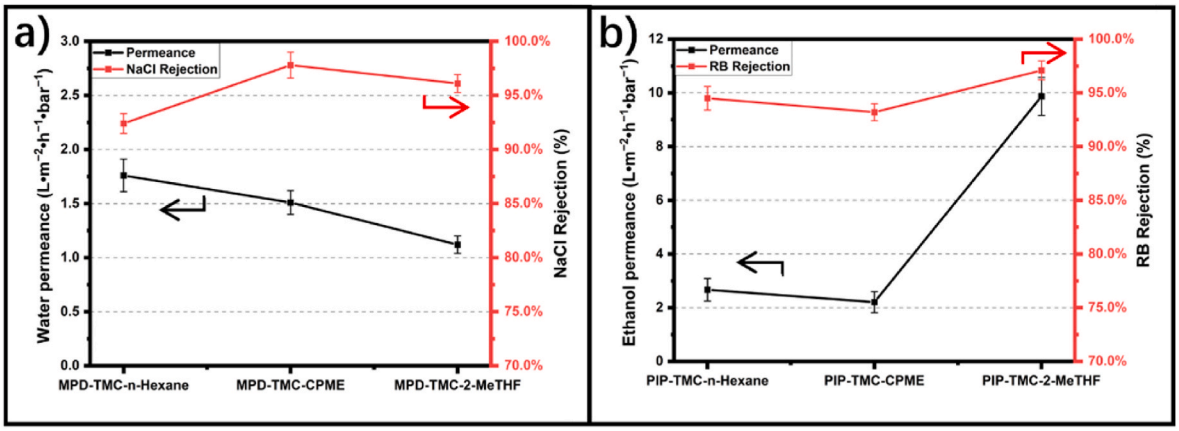

Fig. 6. a) Desalination performance of MDP-TMC polyamide TFC membrane against NaCl water solution; b) OSN performance of PIP-TMC polyamide TFC membrane against RB ethanol solution.

Table 2
Membrane performance comparison.

Membrane type	Organic solvent for IP	Solute	Rejection	Permeance (L m^{-2} h^{-1} bar^{-1})	Ref
MPD-TMC	n-hexane	NaCl	92.4%	1.76	This work
MPD-TMC	n-Hexane	NaCl	90%	1.75	[76]
MPD-TMC	Isoparrafin	NaCl	95%	1.875	[77]
MPD-TMC	Ionic liquid	NaCl	98.2%	0.74	[66]
MPD-TMC	Ionic liquid	NaCl	96.8	1.09	[60]
MPD-TMC	CPME	NaCl	97.8%	1.51	This work
MPD-TMC	Xylene	NaCl	99.8%	1.57	[44]
MPD-TMC	Toluene	NaCl	99.9%	1.59	[44]
PIP-TMC	n-Hexane	RB/EtOH	94.6%	2.67	This work
PIP-TMC	n-Hexane	RB/EtOH	95.9%	2.8	[71]
PIP/PEI-TMC	Ionic liquid	RB/EtOH	98.1%	2.6	[79]
PEI-TMC	n-Hexane	RB/EtOH	99%	3.3	[80]
PA/TiO_2@rGO	n-Hexane	RB/EtOH	97%	3.43	[81]
PIP-TMC-PA6	n-Hexane	RB/EtOH	96%	5	[82]
PEI-TMC	n-Hexane	RB/EtOH	96%	6	[83]
Aramid/PEI	DMSO	RB/EtOH	98.4%	9.1	[84]
PIP-TMC	2-MeTHF	RB/EtOH	97.1%	9.87	This work

4. Conclusions

In this study, we have successfully demonstrated the substitution of a toxic solvent, n-hexane, with more benign solvents such as CPME and 2-MeTHF as the organic phase during interfacial polymerization of polyamides. We showed that these two solvents could be used to fabricate fully and semi-aromatic polyamide and their variants. By using CPME and 2-MeTHF as organic phases, we deposited polyamide selective layers on to the surfaces of porous PES support layers, yielding TFC membranes. Replacing n-hexane with CPME enhanced the fully aromatic MPD-TMC based polyamide TFC with a higher NaCl rejection rate, reaching 97.8% rejection, while the permeance is slightly decreased by 14.2%. Replacing n-hexane with 2-MeTHF enhanced the semi-aromatic PIP-TMC based polyamide TFC with a 3.7-fold higher permeance and 97.1% dye rejection. The increments in solvent permeances did not reduce dye rejection rates during organic solvent nanofiltration. These findings could be beneficial for membrane separations whilst improving the green metrics of membrane fabrication. These promising results could potentially transform the fabrication of TFCs into a more sustainable process.

Author contributions

Shiliang Lin: Conceptualization, Data curation, Formal analysis, Investigation, Methodology, Validation, Visualization, Writing-original draft and Writing-review & editing.

Andrea Correa Semiao: Investigation, Methodology, Writing-original draft and Writing-review & editing.

Yanqiu Zhang: Data curation, Formal analysis, Investigation, Methodology, Validation, and Writing-review & editing.

Lu Shao: Formal analysis, Investigation, Methodology, and Writing-review & editing.

Cher Hon Lau: Conceptualization, Formal analysis, Investigation, Methodology, Resources, Supervision, Project administration, Validation, Visualization, Writing-original draft and Writing-review & editing.

Author agreement/statement

We the undersigned declare that this manuscript is original, has not been published before and is not currently being considered for publication elsewhere.

We confirm that the manuscript has been read and approved by all named authors and that there are no other person who satisfied the criteria for authorship but are not listed. We further confirm that the order of authors listed in the manuscript has been approved by all of us.

We understand that the Corresponding Author is the sole contact for the Editorial process. He/She is responsible for communicating with the authors about progress, submissions of revisions and final approval of proofs.

Declaration of competing interest

The authors declare that they have no known competing financial interests or personal relationships that could have appeared to influence the work reported in this paper.

Data availability

Data will be made available on request.

Acknowledgements

We acknowledge financial funding from the Royal Society International Exchange Grant (grant number: IECS\NSFC\201329). This work was also supported by the National Natural Science Foundation of China (22178076, 22208072).

Appendix A. Supplementary data

Supplementary data to this article can be found online at https://doi.org/10.1016/j.memsci.2023.122281.

References

[1] I. Raheem, N.M. Mubarak, R.R. Karri, N.H. Solangi, A.S. Jatoi, S.A. Mazari, M. Khalid, Y.H. Tan, J.R. Koduru, G. Malafaia, Chemosphere 311 (2022), 137056.
[2] S. Zhao, L. Shen, Front. Chem. 8 (2020), 609774.
[3] A. Al-Karaghouli, L.L. Kazmerski, Renew. Sustain. Energy Rev. 24 (2013) 343–356.
[4] M.G. Buonomenna, J. Bae, Separ. Purif. Rev. 44 (2014) 157–182.
[5] E.M. Rundquist, C.J. Pink, A.G. Livingston, Green Chem. (2012) 14.
[6] F. Liu, L. Wang, D. Li, Q. Liu, B. Deng, RSC Adv. 9 (2019) 35417–35428.
[7] D.L. Francisco, L.B. Paiva, W. Aldeia, Polym. Compos. 40 (2018) 851–870.
[8] Q. Yao, S. Li, R. Zhang, L. Han, B. Su, Separ. Purif. Technol. (2021) 258.
[9] J.A.D. Marquez, M.B.M.Y. Ang, B.T. Doma, S.-H. Huang, H.-A. Tsai, K.-R. Lee, J.-Y. Lai, J. Membr. Sci. 564 (2018) 722–731.
[10] I.-C. Kim, B.-R. Jeong, S.-J. Kim, K.-H. Lee, Desalination 308 (2013) 111–114.
[11] B. Yuan, C. Jiang, P. Li, H. Sun, P. Li, T. Yuan, H. Sun, Q.J. Niu, ACS Appl. Mater. Interfaces 10 (2018) 43057–43067.
[12] A. Dedvukaj, S. Raemdonck, I.F.J. Vankelecom, J. Membr. Sci. (2023) 685.
[13] C.Y. Tang, Y.-N. Kwon, J.O. Leckie, Desalination 242 (2009) 168–182.
[14] X. Cheng, Q. Pan, H. Tan, k. Chen, W. Liu, Y. Shi, S. Du, B. Zhu, RSC Adv. 13 (2023) 22113–22121.
[15] C.Y. Tang, Y.-N. Kwon, J.O. Leckie, Desalination 242 (2009) 149–167.
[16] X. Dong, D. Lu, T.A.L. Harris, I.C. Escobar, Membranes (2021) 11.
[17] G. Szekely, M.F. Jimenez-Solomon, P. Marchetti, J.F. Kim, A.G. Livingston, Green Chem. 16 (2014) 4440–4473.
[18] P. Tomietto, F. Russo, F. Galiano, P. Loulergue, S. Salerno, L. Paugam, J.-L. Audic, L. De Bartolo, A. Figoli, J. Membr. Sci. (2022) 643.

[19] F. Gao, R.X. Bai, F. Ferlin, L. Vaccaro, M.H. Li, Y.L. Gu, Green Chem. 22 (2020) 6240–6257.
[20] P. Noppawan, S. Sangon, P. Chatsiri, N. Khunmood, S. Aintharabunya, N. Supanchaiyamat, A.J. Hunt, RSC Adv. 13 (2023) 2427–2437.
[21] L. Paseta, C. Echaide-Górriz, C. Téllez, J. Coronas, Green Chem. 23 (2021) 2449–2456.
[22] J.M. Luque-Alled, L. Martínez-Izquierdo, P. Gorgojo, C. Téllez, J. Coronas, Chem. Eng. J. 470 (2023), 144233.
[23] W. Li, Z. Yang, W. Yang, H. Guo, C.Y. Tang, AIChE J. (2021) 68.
[24] Z. Ma, L.-F. Ren, D. Ying, J. Jia, J. Shao, Desalination (2022) 539.
[25] C. Ong, G. Falca, T. Huang, J. Liu, P. Manchanda, S. Chisca, S.P. Nunes, ACS Sustain. Chem. Eng. 8 (2020) 11541–11548.
[26] G. de Gonzalo, A.R. Alcantara, P. Dominguez de Maria, ChemSusChem 12 (2019) 2083–2097.
[27] H.H. Khoo, L.L. Wong, J. Tan, V. Isoni, P. Sharratt, Resour. Conserv. Recycl. 95 (2015) 174–182.
[28] E. Yara-Varón, A.S. Fabiano-Tixier, M. Balcells, R. Canela-Garayoa, A. Bily, F. Chemat, RSC Adv. 6 (2016) 27750–27759.
[29] G.N. Ricarte, M.A.Z. Coelho, I.M. Marrucho, B.D. Ribeiro, 3 Biotech 10 (2020) 405.
[30] M.E. Farahat, P. Perumal, W. Budiawan, Y.-F. Chen, C.-H. Lee, C.-W. Chu, J. Mater. Chem. A 5 (2017) 571–582.
[31] Z. Li, L. Ying, P. Zhu, W. Zhong, N. Li, F. Liu, F. Huang, Y. Cao, Energy Environ. Sci. 12 (2019) 157–163.
[32] P. Lei, Y. Mu, Y. Wang, Y. Wang, Z. Ma, J. Feng, X. Liu, M. Szostak, ACS Sustain. Chem. Eng. 9 (2020) 552–559.
[33] S.S. de Jesus, G.F. Ferreira, M.R. Wolf Maciel, R. Maciel Filho, Fuel 235 (2019) 1123–1130.
[34] A.F. Quivelli, F.V. Rossi, C. Alario, F. Sannicolo, P. Vitale, J. Garcia-Alvarez, F. M. Perna, V. Capriati, Molecules 27 (2022).
[35] Á. Díaz-Ortiz, A. de la Hoz, in: J. Alcazar, A. de la Hoz, A. Díaz-Ortiz (Eds.), Flow Chemistry in Drug Discovery, Springer International Publishing, Cham, 2021, pp. 23–70, https://doi.org/10.1007/7355_2021_111.
[36] K. Watanabe, N. Yamagiwa, Y. Torisawa, Org. Process Res. Dev. 11 (2007) 251–258.
[37] S.L. Lin, S.S. He, S. Sarwar, R.A. Milescu, C.R. McElroy, S. Dimartino, L. Shao, C. H. Lau, J. Mater. Chem. A 11 (2023) 891–900.
[38] F. Gao, R. Bai, F. Ferlin, L. Vaccaro, M. Li, Y. Gu, Green Chem. 22 (2020) 6240–6257.
[39] S.-H. Huang, C.-J. Hsu, D.-J. Liaw, C.-C. Hu, K.-R. Lee, J.-Y. Lai, J. Membr. Sci. 307 (2008) 73–81.
[40] Y. Kang, J. Jang, S. Kim, J. Lim, Y. Lee, I.S. Kim, ACS Appl. Mater. Interfaces 12 (2020) 36148–36158.
[41] C.Y.Y. Tang, Y.N. Kwon, J.O. Leckie, Desalination 242 (2009) 149–167.
[42] Z. Jiang, S. Karan, A.G. Livingston, Adv. Mater. 30 (2018), e1705973.
[43] V. Pace, L. Castoldi, A.R. Alcántara, W. Holzer, RSC Adv. 3 (2013).
[44] S.-J. Park, S.J. Kwon, H.-E. Kwon, M.G. Shin, S.-H. Park, H. Park, Y.-I. Park, S.-E. Nam, J.-H. Lee, Polymer 144 (2018) 159–167.
[45] S. Habib, B.E. Larson, S.T. Weinman, Journal of Membrane Science Letters 3 (2023).
[46] S. Yang, J. Wang, Y. Wang, Y. Ding, W. Zhang, F. Liu, Separ. Purif. Technol. (2021) 275.
[47] Y. Li, X. You, R. Li, Y. Li, C. Yang, M. Long, R. Zhang, Y. Su, Z. Jiang, J. Membr. Sci. (2021) 637.
[48] J. Mansouri, S. Huang, A. Agostino, R.P. Kuchel, G. Leslie, C.Y. Tang, A.G. Fane, Desalination (2023) 549.
[49] O. Akin, F. Temelli, Desalination 278 (2011) 387–396.
[50] X. Wei, Y. Peng, W. Fang, Z. Hu, W. Li, S. Zhang, J. Jin, J. Mater. Chem. A 10 (2022) 20424–20430.
[51] Z. Zhang, G. Kang, H. Yu, Y. Jin, Y. Cao, Desalination 466 (2019) 16–23.
[52] M. Shan, H. Kang, Z. Xu, N. Li, M. Jing, Y. Hu, K. Teng, X. Qian, J. Shi, L. Liu, J. Colloid Interface Sci. 548 (2019) 170–183.
[53] P. Sarkar, S. Modak, S. Karan, Adv. Funct. Mater. (2020) 31.
[54] Y. Liang, Y. Zhu, C. Liu, K.R. Lee, W.S. Hung, Z. Wang, Y. Li, M. Elimelech, J. Jin, S. Lin, Nat. Commun. 11 (2020) 2015.
[55] I. Nulens, R. Peters, R. Verbeke, D.M. Davenport, C. Van Goethem, B. De Ketelaere, P. Goos, K.V. Agrawal, I.F.J. Vankelecom, J. Membr. Sci. (2023) 667.
[56] C. Kong, M. Kanezashi, T. Yamomoto, T. Shintani, T. Tsuru, J. Membr. Sci. 362 (2010) 76–80.
[57] C. Kong, T. Shintani, T. Kamada, V. Freger, T. Tsuru, J. Membr. Sci. 384 (2011) 10–16.
[58] T. Kamada, T. Ohara, T. Shintani, T. Tsuru, J. Membr. Sci. 453 (2014) 489–497.
[59] T. Kamada, T. Ohara, T. Shintani, T. Tsuru, J. Membr. Sci. 467 (2014) 303–312.
[60] H. Marien, L. Bellings, S. Hermans, I.F. Vankelecom, ChemSusChem 9 (2016) 1101–1111.
[61] D. Zheng, D. Hua, A. Yao, Y. Hong, X. Cha, X. Yang, S. Japip, G. Zhan, J. Membr. Sci. 636 (2021), 119551.
[62] Z. Ma, L.-F. Ren, D. Ying, J. Jia, J. Shao, Desalination 539 (2022), 115952.
[63] Y. Fang, B. Jiang, Y. Hao, N. Yang, L. Zhang, C. Zhang, Y. Sun, X. Xiao, L. Zhang, J. Membr. Sci. 678 (2023), 121689.
[64] J. Jegal, S.G. Min, K.-H. Lee, J. Appl. Polym. Sci. 86 (2002) 2781–2787.
[65] H. Wang, Q. Zhang, S. Zhang, J. Membr. Sci. 378 (2011) 243–249.
[66] Y. Hartanto, M. Corvilain, H. Mariën, J. Janssen, I.F.J. Vankelecom, J. Membr. Sci. 601 (2020), 117869.
[67] H. Mariën, L. Bellings, S. Hermans, I.F.J. Vankelecom, ChemSusChem 9 (2016) 1101–1111.
[68] H. Hoseinpour, M. Peyravi, A. Nozad, M. Jahanshahi, J. Taiwan Inst. Chem. Eng. 67 (2016) 453–466.
[69] Y. Cui, X.-Y. Liu, T.-S. Chung, Ind. Eng. Chem. Res. 56 (2017) 513–523.
[70] B. Zhao, X. Long, H. Wang, L. Wang, Y. Qian, H. Zhang, C. Yang, Z. Zhang, J. Li, C. Ma, Y. Shi, Colloids Surf. A Physicochem. Eng. Asp. 612 (2021), 125971.
[71] K. Chen, P. Li, H. Zhang, H. Sun, X. Yang, D. Yao, X. Pang, X. Han, Q. Jason Niu, Separ. Purif. Technol. 251 (2020), 117387.
[72] X. Zhang, T. Li, Z. Wang, J. Wang, S. Zhao, J. Membr. Sci. 668 (2023), 121294.
[73] X. Cheng, Y. Qin, Y. Ye, X. Chen, K. Wang, Y. Zhang, A. Figoli, E. Drioli, Chem. Eng. J. 417 (2021), 127976.
[74] G.S. Lai, W.J. Lau, P.S. Goh, A.F. Ismail, Y.H. Tan, C.Y. Chong, R. Krause-Rehberg, S. Awad, Chem. Eng. J. 344 (2018) 524–534.
[75] L. Liu, X. Zuo, J. He, Y. Zhou, J. Xiong, C. Ma, Z. Chen, S. Yu, J. Membr. Sci. 640 (2021), 119867.
[76] H. Zhao, S. Qiu, L. Wu, L. Zhang, H. Chen, C. Gao, J. Membr. Sci. 450 (2014) 249–256.
[77] Z. Yong, Y. Sanchuan, L. Meihong, G. Congjie, J. Membr. Sci. 270 (2006) 162–168.
[78] H. Zhang, Fluid Phase Equil. 403 (2015) 23–29.
[79] A. Yao, D. Hua, Y. Hong, J. Pan, X. Cheng, K.B. Tan, G. Zhan, ACS Appl. Nano Mater. 5 (2022) 18718–18729.
[80] Z. Zha, P. He, S. Zhao, R. Guo, Z. Wang, J. Wang, J. Membr. Sci. 647 (2022), 120306.
[81] H. Abadikhah, E.N. Kalali, S. Behzadi, S.A. Khan, X. Xu, M.E. Shabestari, S. Agathopoulos, Chem. Eng. Sci. 204 (2019) 99–109.
[82] Y.-C. Wang, W.-J. Wang, Q. Wang, Z.-Y. Wang, X.-Y. Yan, L.-L. Zhao, X.-L. Cao, S.-P. Sun, Separ. Purif. Technol. 285 (2022), 120322.
[83] X. Cheng, X. Jiang, Y. Zhang, C.H. Lau, Z. Xie, D. Ng, S.J.D. Smith, M.R. Hill, L. Shao, ACS Appl. Mater. Interfaces 9 (2017) 38877–38886.
[84] Y. Li, S. Yuan, C. Zhou, Y. Zhao, B. Van der Bruggen, J. Mater. Chem. A 6 (2018) 22987–22997.
[85] S.-L. Li, P. Wu, J. Wang, J. Wang, Y. Hu, Desalination (2020) 473.